Chapter 32
Evolution Through Helium Burning: Massive Stars

The evolution of massive stars (stars with $M \gtrsim 8 \cdots 10$) through the phases of central hydrogen and helium burning would be quite similar to that of intermediate-mass stars (Chap. 31) if it were not for a few effects that influence it appreciably and which are specific for this mass range. The fact that the size of the convective core is encompassing large fractions of the star (Fig. 22.7) makes uncertainties connected with the treatment of convection even more important. These are twofold: semiconvection and overshooting, which we introduced already in Sect. 30.4. Furthermore, massive stars are known to have intensive mass loss, which in some cases are able to uncover the cores such that layers with a composition modified by nuclear fusion processes become visible. These are the so-called Wolf-Rayet stars. Finally, massive stars can rotate with surface rotation speeds of up to a few hundred km/s, or to an appreciable fraction of the break-up speed. This leads, as we will see in Chap. 44, to additional mixing processes beyond convective mixing, and further effects. The modelling of massive star evolution therefore becomes quite complicated and uncertain because of these physical effects which are not well understood. We will discuss their general influence in the following.

32.1 Semiconvection

The problem of semiconvection was already introduced and illustrated in Sect. 30.4.2 and Fig. 30.12. It is of particular importance for the evolution of stars above, say, 10 $M_\odot$, and results from the fact that the convective core contains less and less mass during the main-sequence evolution. This "shrinking" of the core is due to the increasing concentration of nuclear energy production, taking place via the CNO cycles, towards the centre with increasing core temperature. It leaves behind a region of varying chemical composition around the convective core, with material that experienced only some amount of nuclear fusion surrounding inner layers, where the conversion of hydrogen to helium proceeded further. In these layers, both the stabilizing molecular gradient ∇_μ and the radiative temperature

R. Kippenhahn et al., *Stellar Structure and Evolution*, Astronomy and Astrophysics Library, DOI 10.1007/978-3-642-30304-3_32, © Springer-Verlag Berlin Heidelberg 2012

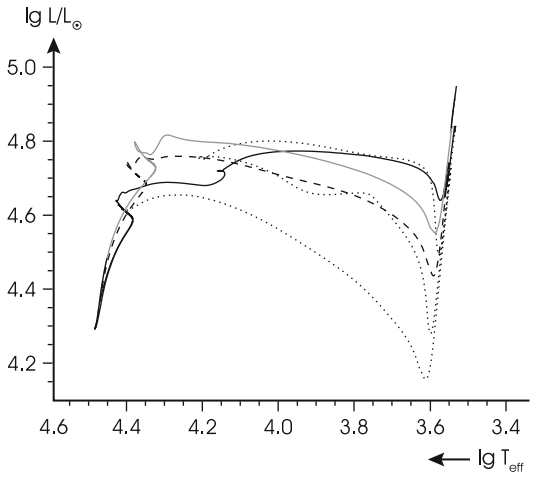

Fig. 32.1 Evolution of a 15 $M_\odot$ star of initial composition $X = 0.70$, $Y = 0.28$, $Z = 0.02$ with different treatments of core convection. The *solid black line* is the resulting evolution if the Schwarzschild criterion is applied, the *dotted* one in case of the Ledoux criterion, with slow semiconvective mixing, and the *dashed* one for the case with the inclusion of overshooting and the Schwarzschild criterion. The *grey solid line*, finally, has been computed with more overshooting and additional mass loss

gradient $\nabla_{\rm rad}$ are strongly oscillating functions of depth, depending on the exact chemical profile left behind by the shrinking core. In numerical models this profile depends on the spatial and temporal resolution of the models and their evolution, but also, for example, on the detailed interpolation in sets of opacity tables. In particular, it is quite important how accurately the varying chemical composition at each position inside the star is represented by these tables. As a consequence of these fluctuating terms in (30.10), the stability condition may be fulfilled in some parts of these critical regions, but not in others. The result is a region above the core with fluctuating radiative and convective layers, the exact structure of which is rather uncertain to compute.

If the Schwarzschild criterion for convection is used, the stabilizing molecular weight gradient in (30.10) is omitted and the layers become convective more easily and earlier in the evolution. This is the situation displayed in the top panel of Fig. 30.12 for a sample calculation of a 15 $M_\odot$ star. Since the separation between the convective core and the semiconvective layers outside of it may be rather small, a connection of both may occur, which "rejuvenates" the core by mixing fresh hydrogen into the burning region. The main-sequence evolution is thus extended and happens at higher luminosities. In Fig. 32.1 we show the resulting evolutionary track in the HR diagram (solid line) of a calculation, in which this effect was avoided. In this case the core helium burning is starting already during the evolution towards the red region, at a temperature of $\log T_{\rm eff} = 4.17$ (we have set, rather arbitrarily, this phase to the point, when the helium luminosity has reached 20 % of the hydrogen

luminosity). This is at an age of 9.35 Myr, and the core helium burning lasts for another 1.43 Myr. At that time the star is beyond the luminosity minimum close to the red (super-)giant region. The onset of core helium burning is connected with the small loop at $\log T_{\rm eff} \approx 4.15$.

The lower panel in Fig. 30.12 and the dotted line in Fig. 32.1 correspond to the case of the Ledoux criterion. In this case the semiconvective layers above the shrinking core mix only slowly, and a more gradual chemical gradient between the hydrogen-exhausted core and the envelope is maintained. This is illustrated in Fig. 32.2, which compares the hydrogen profile at the end of the main sequence for the two criteria for convective stability. In the Ledoux case, the profile in the outer parts of the initially convective core (out to $m/M \approx 0.35$) is very smooth, whereas in the case of the Schwarzschild criterion it shows steps due to the sporadic appearance of localized convective regions.

In the Ledoux case, the main sequence lasts longer for 1.4 Myr, and the helium burning starts only 40,000 years later, at $\log L/L_\odot = 4.41$ and $\log T_{\rm eff} = 3.78$, i.e. after the star has crossed the Hertzsprung gap on a thermal timescale and is approaching the luminosity minimum close to the Hayashi line, along which it quickly ascends within a few 10^4 years. Due to the deep convective envelope the chemical composition is homogeneous down to $m/M \approx 0.25$ (Fig. 32.2, lines showing the helium profile), while in the Schwarzschild case, steps still exist, because at this stage, when the central helium content is 0.48, the star has not yet reached the red giant region.

The most striking difference is the blue loop that the Ledoux model performs during core helium burning. At its hottest extension, the central helium content is reduced to 19 %; it is exhausted when the star is about halfway back to the giant region. This phase lasts for 1.23 Myr, comparable to the duration of central core helium burning in the Schwarzschild case. The fact that stars in that mass range, calculated using the Ledoux criterion for convection and under the assumption of slow semiconvective mixing, first become red giants and then perform blue loops was very crucial in explaining the pre-explosion evolution of the progenitor of supernova SN1987A, a star known as Sanduleak $-69°202$ (see, e.g. Woosley et al. 1988; Langer 1989).

32.2 Overshooting

The effect of overshooting on the interior evolution of the same star is visible in the middle panel of Fig. 30.12. The evolutionary path in the HR diagram (Fig. 32.1) is shifted in a similar way as was shown in Fig. 31.2b, i.e. to higher luminosities. Due to the enlarged convectively mixed core, central hydrogen burning lasts now for 12.12 Myr, i.e. about 2.8 Myr (30 %) longer than for the case without overshooting. This corresponds roughly to the increased amount of fuel for the nuclear fusion, which can also be recognized from the hydrogen profile shown in Fig. 32.2. Note also that overshooting has the additional effect of creating a

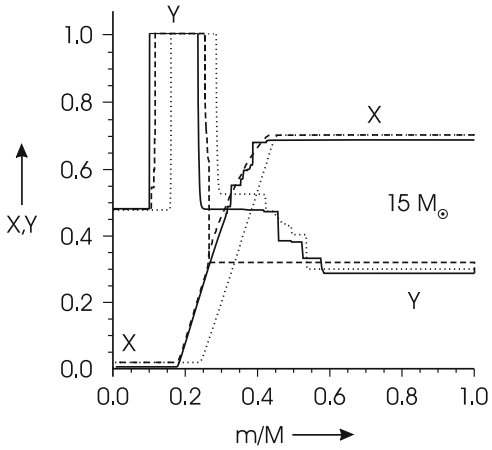

Fig. 32.2 Chemical composition profiles for selected models along the evolution shown in Fig. 32.1. Shown are the hydrogen and helium mass fractions (indicated by the usual symbols X and Y) as function of relative mass. The *solid lines* refer to the models calculated with the Schwarzschild criterion, the *dashed lines* to those with the Ledoux criterion for convection, and finally the *dotted* ones to the case with convective overshooting. The models were taken at the end of the main sequence when the central hydrogen abundance had been reduced to 0.01, and during core helium burning, when the central helium abundance is at 0.48

smooth chemical profile. The increase in luminosity of $\triangle \log L/L_{\odot} \approx 0.11$ at the end of the main sequence agrees well with a simple estimate using (20.20), which predicts $L \sim \mu^4$, where μ is the mean molecular weight obtained from that of the hydrogen-rich envelope and of the helium-rich core. μ increases from 0.83 to 0.90 when overshooting is enlarging the core, and therefore $\log L$ by approximately 0.14. Core helium burning starts again halfway through the crossing of the HR diagram, but without a visible feature in the track, and lasts for another 1.2 Myr. Although overshooting enlarges the convective helium-burning core, too, the increased luminosity leads to an overall reduced duration of this nuclear phase. This star does not perform any loop. This agrees with the similarity of the helium profile with that of the Schwarzschild case (Fig. 32.2).

Overshooting is even more important for more massive stars. Figure 32.3 shows evolutionary tracks for stars of 40 and 50 $M_{\odot}$. For reference, the solid track of the 40 $M_{\odot}$ star was calculated without any overshooting, while the dotted grey line does include it. The broadening of the main-sequence phase and the increase in luminosity are obvious. The core hydrogen burning phase is extended from 4.47 to 4.69 Myrs, too. The models for the 50 $M_{\odot}$ star all include overshooting, but differ in the criterion for convection. One realizes that until the end of core hydrogen burning (after 4.14 respectively 4.12 Myrs), both tracks are almost identical, but differ afterwards, when the newly established hydrogen shell encounters the hydrogen profile, which, due to the use of the Schwarzschild (dotted line) or Ledoux (solid line) criterion, is different. As we discussed in the previous section, the treatment of convection influences strongly the post-main-sequence evolution!

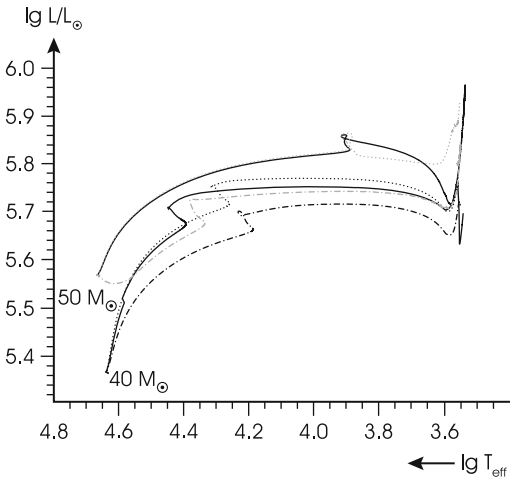

Fig. 32.3 Evolution of 40 and 50 $M_\odot$ stellar models calculated with various assumptions concerning semiconvection, overshooting, and mass loss. For the 40 $M_\odot$ star three cases are shown: one with neither overshooting nor mass loss using the Schwarzschild criterion for convection (*black solid track*), one with strong overshooting (*grey dotted*), and one with additional mass loss (*black dot dashed*). In total, this last model loses about 5 $M_\odot$. The *black solid line* for the 50 $M_\odot$ star refers to a case with overshooting and mass loss; the Ledoux criterion for convection was used here. For comparison, using the Schwarzschild criterion results in the *grey dotted line*. Finally, the *grey dash-dotted line* corresponds to a case with significantly enhanced mass loss. The final mass of this model is 28 $M_\odot$ compared to 37.5 and 42.4 $M_\odot$ in the former cases

32.3 Mass Loss

In addition to the complications of the interior evolution due to convection, the evolution of massive stars is also much stronger influenced by mass loss due to stellar winds than that of stars of low and intermediate mass. These strong stellar winds are driven by the radiation field and therefore increase with luminosity and effective temperature (the energy density of radiation scales with $T_{\rm eff}^4$). For a review of winds from hot stars, see Kudritzki and Puls (2000). In the following we used the empirical mass loss formula by Vink et al. (2001) in our models.

In Fig. 32.1 (grey solid line) we show the evolution of the 15 $M_\odot$ model when mass loss is added and the amount of overshooting is increased even further, to now about 0.3 $H_{\rm P}$. Accordingly, luminosity increases even further, and the main-sequence phase extends over 12.8 Myr. The mass loss rate on the main sequence is of the order of $1 - 2 \times 10^{-8}\ M_\odot$/year and drops by a factor of a few when the star gets cooler. At the end of helium burning 1.15 $M_\odot$ is lost due to stellar winds. Since the amount of mass loss is below 10 % of the initial mass, the influence on the track, when compared to the case with overshooting, but no mass loss (dashed), is very small.

This is different for the two stars of Fig. 32.3. The 40 $M_\odot$ star, when calculated with mass loss (black dot-dashed line), loses mass at a level close to $10^{-6}\,M_\odot$/year, which amounts, over the main-sequence lifetime of 4.54 Myrs to a reduction to 35.52 $M_\odot$. Since the mass loss timescale is much longer than the nuclear timescale, the star can always adjust to the reduced mass and evolves at any time similar to a star of the same instantaneous constant mass. Note, however, that the width of the main-sequence phase, that is the effective temperature of the "hook" indicating the end of core hydrogen burning is very similar to that of the track without mass loss. The convective core of the star is not influenced very much by the mass loss from the stellar surface. Until the end of core helium burning, the star loses only a further 0.03 $M_\odot$; this is due to the short duration of this phase and the cooler stellar temperatures, which reduce the mass loss rate by more than an order of magnitude.

All calculations of the 50 $M_\odot$ star have been done with mass loss. However, in the case shown by the grey dash-dotted line the mass loss rate by Vink et al. was artificially enhanced by a factor 3. While the stellar mass in the cases with normal mass loss amounts to 42.5 $M_\odot$ after the main-sequence, here the model loses 12 $M_\odot$ over 4.47 Myrs. Mass loss after the main sequence is negligible in all cases. Since this enhanced mass loss is so strong, the star can no longer evolve unperturbed. One can see this in the early part of the main sequence: instead of increasing in luminosity, the track bends down trying to follow a sequence of unevolved stars of decreasing mass. Only during the second half of core hydrogen burning, when the nuclear timescale is further reduced, the usual evolution proceeds, but at lower luminosity and also with a smaller extension of the main sequence. Indeed, the convective core is smaller than in the cases with normal mass loss (17 instead of 27 $M_\odot$ in this phase; compare this to 22 $M_\odot$ of the 40 $M_\odot$ star with Schwarzschild criterion, the evolution of which resembles most closely this one).

The maximum mass loss rate is $5 \times 10^{-6}\,M_\odot$/year for the last case presented. With even more extreme mass loss, up to $10^{-4}\,M_\odot$/year and above, the track would even turn around and the star evolve to temperatures higher than the main sequence (compare this to the generalized main sequences of Sect. 23.3 for large values of q_0). During this evolution, the wind would uncover nuclear-processed layers of the star: first hydrogen-rich layers with high nitrogen abundance (from CNO-burning), later helium-rich layers, and even later possibly carbon-rich, hydrogen-free layers that experienced helium burning. These different surface compositions define the sequence of different types of Wolf-Rayet stars (WN, WC). Such models have been computed and presented by, for example, Maeder and Meynet (1987). However, stars with such strong winds can no longer be considered as having an optically thin atmosphere on top of the opaque interior. Instead, interior, atmosphere, circumstellar envelope and hot, fast stellar wind should be treated together and consistently (see, e.g. Schaerer 1996).

The evolution of massive stars is further influenced significantly by rotation and the mixing of the interior induced by rotation (see Chap. 43). Massive stars are known to rotate with surface velocities of several hundred km/s, sometimes close to break-up velocities. Modelling rotating stars is an active field of research going beyond the scope of this book. Therefore we refer the reader to the monograph by Maeder (2009)